CORRELATED SCANNING/TRANSMISSION ELECTRON MICROSCOPY AND OXYGEN ISOTOPE IMAGING STUDY OF ISOTOPICALLY HETEROGENEOUS ANORTHITE IN E60, A FORSTERITE-BEARING TYPE B CAI FROM EFREMOVKA CV3 CHONDRITE. K. K. Ohtaki[1], K. Nagashima[1], J. P. Bradley[1], A.N. Krot[1] and H. A. Ishii[1], [1] Hawai'i Institute for Geophysics and Planetology, University of Hawai'i at Mānoa, Honolulu, HI 96822, USA (kohtaki@hawaii.edu)

Introduction: Most amoeboid olivine aggregates (AOAs) and Ca,Al-rich inclusions (CAIs), both non-igneous and igneous, from metamorphosed CV3.1–3.6 chondrites exhibit O-isotope heterogeneity: hibonite, spinel, Al-diopside, and forsterite have solar-like ^{16}O-rich compositions ($\Delta^{17}O \sim -25‰$); anorthite, melilite, perovskite, some Al,Ti-diopsides, grossite, Zr- and Sc-rich oxides and silicates are ^{16}O-depleted to various degrees [1–10]. In AOAs and texturally fine-grained CAIs, O-isotope heterogeneity appears to be mineralogically-controlled and could have resulted from post-crystallization O-isotope exchange during fluid-rock interaction on the CV parent asteroid [10,11]. For fluffy Type A CAIs and coarse-grained igneous Type B CAIs several mechanisms of O-isotope heterogeneity are being discussed in the literature. These include: (*i*) condensation in a gaseous reservoir with variable O-isotope composition [e.g. 7], (*ii*) partial melting and O-isotope exchange with the surrounding nebular gas of variable O-isotope composition [e.g. 2,9], and (*iii*) O-isotope exchange during aqueous fluid–rock interaction on the CV parent asteroid [5,8].

Kawasaki *et al*. [9] reported heterogeneous O-isotope distribution in a Type B CAI from Vigarano (CV3.1–3.4 breccia) and concluded that it resulted from gas-melt O-isotope exchange during cyclic change between ^{16}O-rich and ^{16}O-poor compositions of the nebular gas surrounding the CAI melt during its crystallization. Nagashima *et al.* [6] reported micron scale O-isotope heterogeneity in anorthite in the forsterite-bearing Type B CAI E60 from Efremovka ($CV_{reduced}$3.1–3.4), and suggested that it resulted from isotopic exchange during partial melting and recrystallization based on the sharp O-isotope boundary. In this report, another anorthite grain in E60 with heterogeneous isotope distribution was investigated with a scanning/transmission electron microscope (S/TEM) and energy dispersive spectroscopy (EDS), and possible mechanisms of O-isotope exchange are considered.

Experimental: Oxygen isotopographs were collected on a polished thick section of E60 using UH Cameca ims1280+SCAPS [6]. A thin section of the region having O-isotope boundaries was prepared for S/TEM (UH FEI Titan 300 keV) using standard focused ion beam (FIB) preparation methods (UH FEI Helios NanoLab 660).

Results and discussion: Heterogeneous O-isotope distribution was observed in several regions in E60. Fig. 1 shows an isotopically heterogeneous anorthite grain adjacent to a uniformly ^{16}O-poor melilite. The anorthite is mostly ^{16}O-rich but has a ^{16}O-poor stripe in the middle; both types of anorthite are uniform in elemental composition. A secondary electron image (Fig. 1c) aligned with the isotope image reveals cracks aligned with the ^{16}O-poor stripe. We note that these cracks are fine and difficult to see in the ion images.

The TEM image in Fig. 2 shows that cracks on the surface propagate through the FIB section. Electron diffraction from each part of the sample indicates that the section consists of two major anorthite crystals, 1 and 2, with two different orientations. Within each crystal, there are bands with slightly different lattice parameters. Stacking fault formation is commonly observed in melt-crystallized anorthite [12,13]. Since these crystallographic defects are seen in both the ^{16}O-poor and ^{16}O-rich regions, they are unlikely the cause of the heterogeneous O-isotope distribution. Crack 2 has closed voids and a linear interface, indicating that it experienced annealing with crystal 2 to equilibrate the interface. In the rims of the voids, excess oxygen above stoichiometric anorthite was detected.

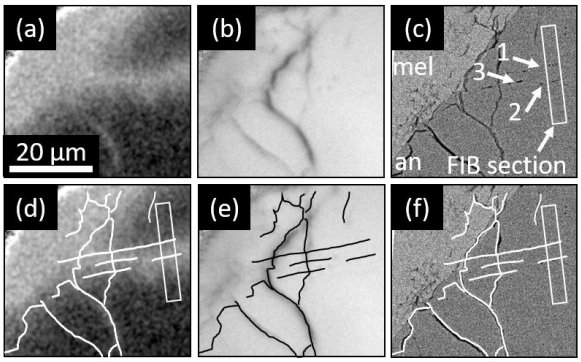

Fig.1 *Oxygen isotope and simultaneous Si^-/O^- images and corresponding SEM image. (a) δ^{18}O-isotopograph. Dark regions are ^{16}O-rich. (b) Si^-/O^- image. (c) SEM image after isotope imaging. 1, 2 and 3 indicate cracks. (d)-(f) Images with outlines along cracks. The white box indicates the FIB section position. an=anorthite; mel=melilite.*

Crack 1 likely postdates crack 2 since it does not exhibit annealed structure. Aluminous pyroxene occupies the bottom half of crack 1; a porous region at the

surface - where the isotopograph in Fig. 1a was obtained - also has excess oxygen that cannot be stoichiometrically accommodated, and carbon was also detected. Oxygen and carbon may be attributable to terrestrial alteration. The crack at the bottom of the image in Fig. 1a is also ^{16}O-poor as seen in Fig. 1b and is filled by carbonate, very likely formed by terrestrial weathering.

It is possible that partial melting and O-isotope exchange, perhaps centered along the boundary between the two crystal orientations at crack 2, are the source of the wide ^{16}O-poor stripe. However, our observations do not strongly support this possibility. The anorthite and melilite share a linear interface that would require partial melting of only of a portion of the anorthite and epitaxial recrystallization, leaving just void spaces. In addition, based on the melting temperatures, Al-Ti-diopside should also have melted but does not show ^{16}O-poor composition in E60, a long-standing puzzle [e.g., 4].

A second, and perhaps more likely, possibility is that ^{16}O-poor fluid or vapor entered through microcracks and exchanged oxygen with the surrounding anorthite and left ^{16}O-poor material in cracks. Hydrothermal alteration is suspected because both cracks 1 and 2 have excess oxygen, although it may be due to terrestrial weathering. In the specific case of the cross-section through the ^{16}O-poor stripe in the anorthite in E60, crack 3 did not penetrate deep enough to intersect the FIB section in the middle of crack 1 and 2 (Fig. 1c), but it falls in the ^{16}O-poor stripe. The heterogeneous isotope distribution in this sample may be due to oxygen exchange with ^{16}O-poor fluid via crack 1, 2 and/or 3 that had access to a ^{16}O-poor reservoir, presumably via aqueous fluid on the parent asteroid. This scenario seems plausible as the oxygen self-diffusion rate in anorthite under hydrothermal conditions [14] allows O-isotope exchange over 10 μm within 1−100K years under 100-300˚C. This requires very limited or no metasomatism in this region since no extra phases are present at the crack 1 or 2 boundaries.

References: [1] Clayton, R. N. *et al. Earth Planet. Sci. Lett.* **34**, 209–224 (1977). [2] Yurimoto, H. *et al. Science* **282**, 1874–1877 (1998). [3] Yoshitake, M. *et al. GCA* **69**, 2663–2674 (2005). [4] Yurimoto, H. *et al.* In *Oxygen in the Solar System* (ed. MacPherson G. J.), *Rev. Mineral. Geochem.* **68**, 141–187 (2008). [5] Krot, A. N. *et al. GCA* **72**, 2534–2555 (2008). [6] Nagashima, K. *et al. LPSC* **41**, #2255 (2010). [7] Kawasaki, N. *et al. Meteorit. Planet. Sci.* **47**, 2084–2093 (2012). [8] Kawasaki, N. *et al. GCA* **169**, 99–111 (2015). [9] Kawasaki, N. *et al. GCA* **221**, 318–341 (2018). [10] Krot, A. N. *et al. GCA*, in press (2018). [11] Krot A. N. *et al. LPSC* **49**, #2416 (2018). [12] Carpenter, M. *Am. Mineral.* **76**, 1110–1119 (1991). [13] Xu, H. *et al. Am. Mineral.* **82**, 125–130 (1997). [14] Giletti B. J. *et al. GCA* **42**, 45-57 (1978).

Acknowledgments: This research is supported by NASA grants NNX14AI48G to HAI and NNX15AH44H to KN.

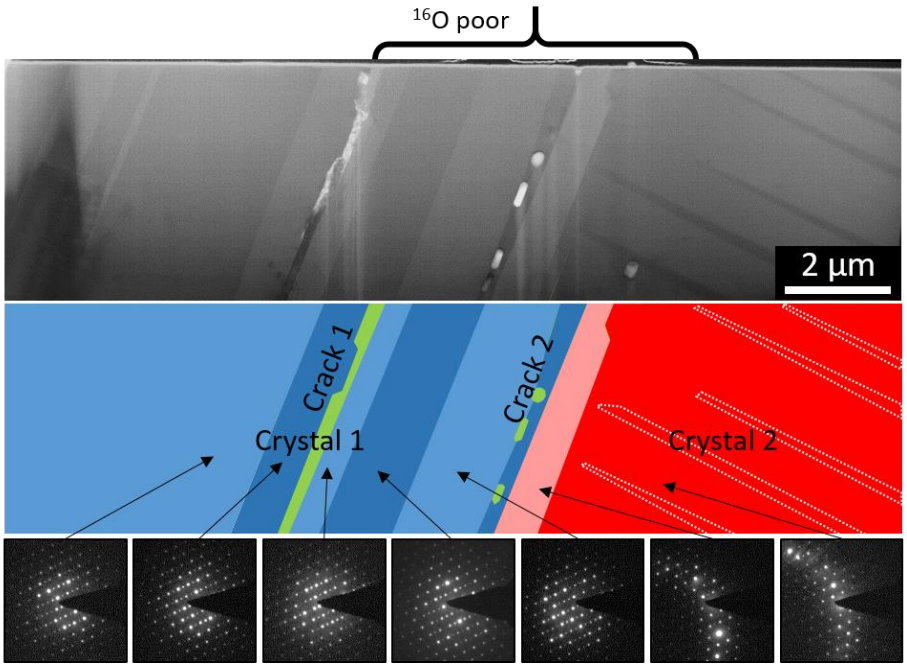

Fig. 2. *STEM BF image of the FIB section through the ^{16}O-poor stripe in anorthite and an illustration of crystal orientation. Crystal 1 (blue) and Crystal 2 (red) have different crystal orientations as seen in the inserted electron diffraction patterns. Crack 1 and 2 correspond to those in Fig. 1c.*